ISSN No. 2321-2705 | DOI: 10.51244/IJRSI |Volume XII Issue II February 2025

Anticancer Evaluation and Angiogenic Inhibition of Atis *(Annona squamosa Linn.)* Seed Extract Against A549 Human Lung Adenocarcinoma through MTT Assay and Pharmacokinetic Analyses

Juliah Bless E. Bontilao, Niña Kate T. Garrido, Kiara Leigh L. Manzo, Sherwin S. Fortugaliza

Davao City National High School

DOI: https://doi.org/10.51244/IJRSI.2025.12020094

Received: 06 February 2025; Accepted: 18 February 2025; Published: 25 March 2025

ABSTRACT

In 2022, lung cancer was the most diagnosed cancer globally, with approximately 2.5 million new cases, accounting for 12.4% of all malignancies. Non-small cell lung cancer (NSCLC), comprising nearly 90% of cases, includes lung adenocarcinoma as the most common subtype, responsible for about 30% of all lung cancers. This study evaluated the anticancer potential of Annona squamosa Linn. (Atis) seed extract against A549 human lung adenocarcinoma cells using an in vitro MTT assay and in silico methods, including PASS prediction, ADMET analysis, and molecular docking simulations. The MTT assay tested concentrations of 12.5, 25, 50, and 100 µg/ml, with Doxorubicin as the positive control. Results showed that 100 µg/ml of Atis seed extract exhibited the highest cytotoxicity against A549 cells, comparable to the positive control. In silico analysis further revealed strong inhibitory potential, with binding affinities ranging from -5.8 to -9.2 kcal/mol. These findings suggest that Atis seed extract is a promising candidate for lung cancer treatment, warranting further investigation.

Keywords: A549 Human Lung Adenocarcinoma, MTT Assay, PASS, ADMET, Molecular Docking, Annona squamosa Linn.

INTRODUCTION

Cancer remains one of the world's most significant health challenges. Despite advancements in treatment, a 15% increase in cases over 29 years indicates limited success in controlling the disease (Roser & Ritchie, 2024). In the Philippines, cancer is a leading cause of death, with over 150,000 recorded cases and 90,000 fatalities in 2020 (Dee et al., 2022).

Lung cancer was the most diagnosed cancer in 2022, with approximately 2.5 million new cases, accounting for 12.4% of all malignancies worldwide (Bray et al., 2024). In the Philippines, it ranks first among cancer-related deaths, primarily due to smoking. Around 80% of the 1.3 billion smokers worldwide come from low- and middle-income countries (LMICs) like the Philippines, where over 25% of the adult population uses tobacco, increasing their risk of lung cancer (Suanes et al., 2023).

Non-small cell lung cancer (NSCLC) accounts for nearly 90% of lung cancer cases and progresses more slowly than small cell lung cancer (SCLC). Lung adenocarcinoma, the most common NSCLC subtype, represents 30% of all lung cancers and 40% of NSCLC cases (Types of Lung Cancer: Common, Rare, Aggressive & More, n.d.).

Angiogenesis, the formation of new blood vessels, is essential for tumor growth and cancer cell proliferation. These vessels supply nutrients and oxygen to tumors, allowing them to expand and spread to surrounding tissues (Angiogenesis Inhibitors, 2018).

Common cancer treatments include surgery, chemotherapy, radiation, transplants, immunotherapy, hormone therapy, targeted drug therapy, and clinical trials (Bonvissuto, 2024). However, due to high costs, many individuals turn to traditional herbal medicine, though clinical evidence on its effectiveness remains inconsistent (Asiimwe et al., 2021).

ISSN No. 2321-2705 | DOI: 10.51244/IJRSI |Volume XII Issue II February 2025

Annona squamosa (Atis), commonly known as custard apple in the Philippines, has gained attention for its therapeutic potential. Various parts of the tree have been used in traditional medicine (Vyas et al., 2012). Custard apple seeds, in particular, have shown promising pharmacological properties, including anticancer activity. Studies suggest their efficacy in treating leukemia, liver, prostate, pancreatic, and cervical cancers, with annonaceous acetogenins exhibiting strong anticancer effects (Chen et al., 2011).

This study evaluates the anticancer properties of Annona squamosa (Atis) seed extract using in vitro MTT assay, PASS prediction, ADMET analysis, and molecular docking simulations. Specifically, the researchers aim to:

1. **Anticancer Assessment.** Evaluate the performance of the *Annona squamosa Linn.* seed extract using in-vitro MTT Assay.

2. **Assessment of Phytochemicals.** Evaluate the selected 11 phytochemicals from *Annona squamosa* through Lipinski's Rule of 5, PASS Prediction, and ADMET Analysis.

3. **Molecular Docking Simulation.** Molecular Docking will be used for the assessment of the compounds' ability to inhibit the growth of the Vascular Endothelial Growth Factor (VEGF, PDB: 1VPP) and the Epidermal Growth Factor Receptor (EGFR, PDB: 1M17) proteins.

METHODS

A. Collection and Extraction of Plant Materials

The researchers acquired the unripe Atis *(Annona squamosa Linn.)* fruits at Landmark 3 Subdivision, Sasa, Davao City. The Atis sample was then sent to Ateneo de Davao University for the speciation and was authenticated and identified by Sir Abdul Aziz L. Juhuri.

Figure 1.Atis Plant Sample

The unripe seeds were separated from the fruit and were water-washed, dried by air and then pulverized (to 1.0 mm) in a Wiley mill. 100 grams of the pulverized unripe seeds were then extracted in 200 milliliters of 95% ethanol. Periodically, the suspension was stirred to promote consistent extraction.

Figure 2. Air-Dried Atis Seeds

ISSN No. 2321-2705 | DOI: 10.51244/IJRSI |Volume XII Issue II February 2025

Figure 3. Atis Seeds Subjected to 95% Ethanol

Figure 4. Atis Seed Extract with Ethanol

The supernatant was left aside after a 5-day period and vacuum-filtered. After, the filtered supernatant was mixed to create approximately 250 milliliters of extract solution. Finally, the solution was concentrated at 35°C in a rotary evaporator operating under vacuum.

Figure 5. Atis Seed Extract undergoing Rotary Evaporation

ISSN No. 2321-2705 | DOI: 10.51244/IJRSI |Volume XII Issue II February 2025

Figure 6. Atis Seed Extract after Rotary Evaporation

B. Methyl Thiazolyl Tetrazolium (MTT) Assay

The MTT assay, also known as the 3-(4,5-dimethylthiazol-2-yl)-2,5-diphenyl tetrazolium bromide assay, is a commonly used colorimetric method to measure cell viability and metabolic activity. Introduced by Mosmann in 1983, it has become a standard tool in cell biology for determining the cytotoxic effects of drugs and other compounds on different cell types (Van Meerloo et al., 2011).

Table 1. *Ratios for the Plant Extracts for MTT Assay*

Treatments	**Atis Seed Extract**
Treatment 1	12.5 µg/ml
Treatment 2	25 µg/ml
Treatment 3	50 µg/ml
Treatment 4	100 µg/ml
Positive Control	Doxorubicin

Table 1 shows the treatments with different concentrations of Atis (*Annona squamosa Linn.*) Seed Extract: 12.5, 25, 50 and 100 µg/ml. The treatments also included the positive control group, which is the Doxorubicin (Amaani & Dwira, 2018).

The Atis Seed Extract was sent to the University of the Philippines - Mindanao College of Science and Mathematics (CSM) Laboratory for an MTT Assay wherein all treatments were performed in triplicate and were independently repeated thrice. The assay had a final concentration of 12.5, 25, 50, and 100 µg/ml. Doxorubicin served as the positive control group and DMSO as the vehicle control.

The percent growth inhibition was calculated using the formula below:

$$\% \text{ Inhibition} = \left(100 - \frac{\text{Absorbance of sample - Absorbance of blank control}}{\text{Absorbance of vehicle control - Absorbance of blank control}}\right) \times 100$$

Data Analysis

The absorbance of each well was read using a microplate reader at 570 nm. The results obtained from the percent inhibition of the Atis Seed Extract against A549 Cancer Cell Lines were expressed in medians and standard

ISSN No. 2321-2705 | DOI: 10.51244/IJRSI |Volume XII Issue II February 2025

deviations. Additionally, the IC50 values of the percent inhibitions of the different concentrations and the controls were plotted using graphs following the trendlines of the concentrations between which 50% mean inhibition falls under.

Proper Waste Disposal

The researchers ensured that proper disposal of waste was observed. All disposable materials, excluding materials that were not autoclave safe (e.g. plastics), handled in this study undertook autoclaving before being properly discarded.

C. PASS Prediction

PASS (Prediction of Activity Spectra for Substances) is a computational tool used to predict the biological activity of chemical compounds based on their structure. It estimates the probability of a compound showing specific pharmacological or toxicological activities, aiding in drug discovery by narrowing down potential candidates for further testing (Lagunin et al., 2014). Referring to the study by Lagunin et al. (2014), PASS software applies structure-activity relationship (SAR) analysis, comparing molecular features of compounds with a vast database to predict activities. PASS is used to predict the biological activities of the ligands under study, particularly focusing on anti-angiogenesis or other relevant biological activities.

Figure 7. Image of PASS Online Interface

Figure 8. Sample list of Biological Activity Spectra

All Pa>Pi Pa>0,3 Pa>0,7 ok

Pa	Pi	Activity
0,876	0,003	Neurotransmitter uptake inhibitor
0,802	0,007	Nicotinic alpha4beta4 receptor agonist
0,790	0,006	Antidyskinetic
0,763	0,004	MAP kinase stimulant
0,762	0,004	Leukopoiesis stimulant
0,745	0,003	Antiparkinsonian, rigidity relieving
0,746	0,004	Muscle relaxant
0,745	0,012	Respiratory analeptic
0,751	0,027	Antineurotic
0,719	0,029	Nicotinic alpha6beta3beta4alpha5 receptor antagonist

D. ADMET Analysis

ADMET (Absorption, Distribution, Metabolism, Excretion, and Toxicity) evaluation is essential in drug development, providing insights into pharmacokinetics and minimizing errors in drug discovery. The process begins with data acquisition, including SMILES codes of phytochemicals, followed by computational analysis using tools like DEEP-PK and pkCSM to predict pharmacokinetic properties (Raju et al., 2021).

ISSN No. 2321-2705 | DOI: 10.51244/IJRSI |Volume XII Issue II February 2025

Advancements in computational ADMET analysis have enhanced the accuracy of toxicity and bioavailability predictions. By integrating molecular descriptors and machine learning models, these tools improve drug-likeness evaluation, reducing late-stage failures in development (Raju et al., 2021).

Figure 9. Image of sample Deep-PK results

Figure 10. Image of sample pkCSM results

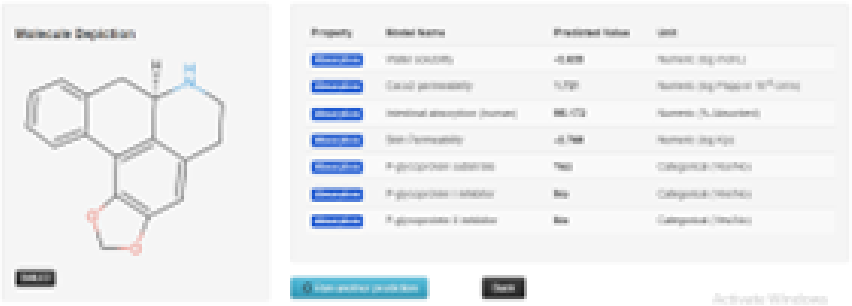

E. Molecular Docking

Molecular docking is a computational method used to predict interactions between a ligand and a macromolecular target, typically a protein. It plays a crucial role in drug design and structural biology by providing atomic-scale insights into drug-target binding (Dar & Mir, 2017).

Screening and Preparation of Phytocompounds from Annona squamosa Linn.

Twenty-nine major compounds from *Annona squamosa* Linn. seeds (Pandey & Barve, 2011) were tested, with eleven phytochemicals retrieved from PubChem. These compounds were screened using Lipinski's rule of five via SwissADME (http://www.swissadme.ch) to evaluate their drug-likeness.

Lipinski's rule states that an orally active drug typically has at most one deviation from these criteria: ≤5 hydrogen bond donors, ≤10 hydrogen bond acceptors, a molecular mass <500 Daltons, and a logP (ClogP) ≤5 (Karami et al., 2022; Olatunde et al., 2022). This assessment confirmed each compound's bioavailability, solubility, and chemical stability for potential pharmaceutical use.

Compounds passing Lipinski's test proceeded to docking simulations using Autodock Vina. Their SDF files were converted to PDB format via PyMOL, prepared in MGL AutodockTools, and optimized with Gasteiger charges and torsional degrees of freedom. The final structures were saved as PDBQT files for docking.

Preparation of A549 Human Lung Adenocarcinoma Receptor VEGF (1VPP) and EGFR (1M17)

The 3D structure of the target proteins (RCSB PDB IDs: 1VPP and 1M17) was downloaded as 3D models from the RCSB Protein Data Bank (https://www.rcsb.org/) in PDB format. After downloading the PDB files, it underwent energy minimization (Tuli et al., 2022) on the Swiss PDB viewer. Then, it was exported to MGL AutodockTools for preparation. Water molecules were deleted, and polar hydrogens and Kollman charges were added and evenly distributed throughout the protein. The modified protein file was saved as a PDBQT file to be accessed by Autodock Vina.

ISSN No. 2321-2705 | DOI: 10.51244/IJRSI |Volume XII Issue II February 2025

Figure 11. 3d Model of A549 Human Lung Adenocarcinoma Receptor VEGF (1VPP)

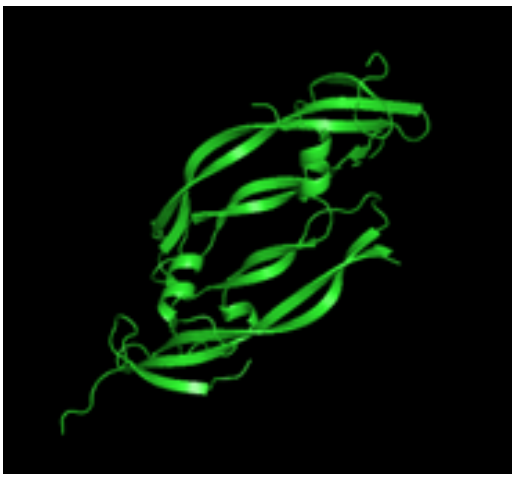

Figure 12. 3d Model of A549 Human Lung Adenocarcinoma Receptor EGFR (1M17)

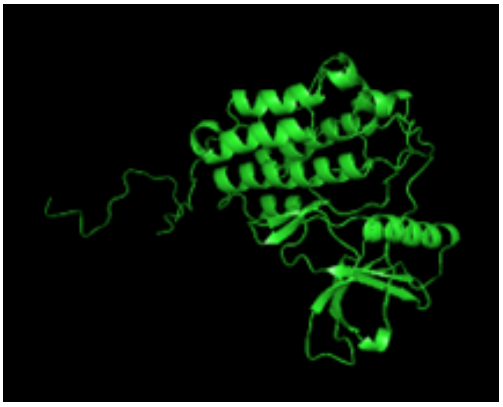

Receptor Grid Box Manual Generation

CASTp was used to predict the 1VPP VEGF and 1M17 EGFR protein's active binding residues (Ali et al., 2018). By utilizing MGL AutodockTools with Autodock Vina, the receptor grid area was calculated. Ali et al. (2018) reduced the binding site size to 40x40x40 Angstrom in order to reduce the likelihood that the software would produce less accurate results and binding outcomes that weren't essential. The coordinates of the grid box's center (x: 2.313; y: 19.998; z: 1.11) and its dimensions (40x40x40) were recorded in a text document for the configuration file, following the default protocol's settings for exhaustiveness level and energy range.

Figure 13. Active binding site of 1VPP shown in CASTp

ISSN No. 2321-2705 | DOI: 10.51244/IJRSI |Volume XII Issue II February 2025

Figure 14. Active binding site of 1M17 shown in CASTp

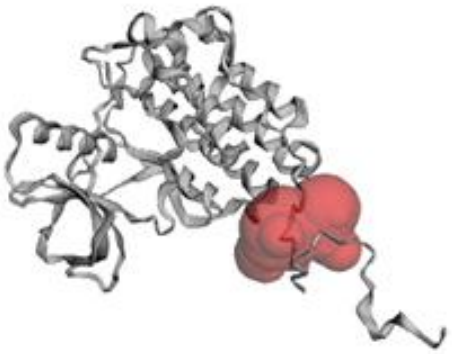

Figure 15. A549 Human Lung Adenocarcinoma Receptor VEGF (1VPP) grid box visualization through MGL Autodock Tools v. 1.5.7

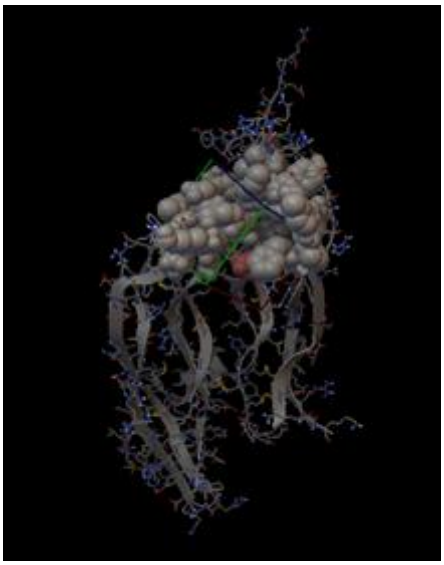

Figure 16. A549 Human Lung Adenocarcinoma Receptor EGFR (1M17) grid box visualization through MGL Autodock Tools v. 1.5.7

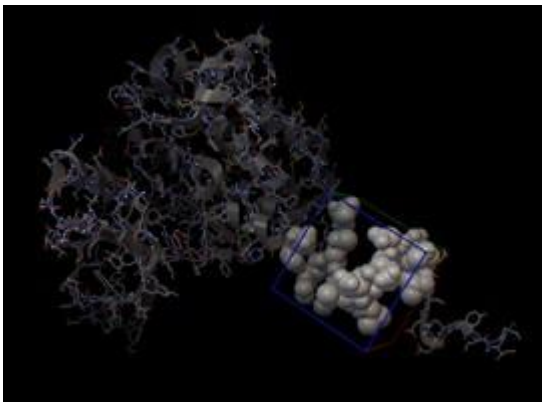

Docking and Analysis

The docking analysis and simulation occurred once the optimized ligands, protein, and configuration files were saved in the same folder. The process occurred through the Command Prompt of Windows 10 and 11 systems. The Autodock Vina software for docking was utilized through the computer's Command Prompt. The location

ISSN No. 2321-2705 | DOI: 10.51244/IJRSI |Volume XII Issue II February 2025

was transferred to the folder's directory, where the ligand, protein, and configuration files were stored. Then the code:

"C:\Program Files (x86)\The Scripps Research Institute\Vina\vina.exe" --receptor protein.pdbqt --ligand [ligand.pdbqt] --config [config.txt] --log [log.txt] --out [output.pdbqt]"

was written in the prompt for the computation. This docking was done, and the binding affinities of the molecules docked to A549 Human Lung Adenocarcinoma Receptors, VEGF (PDB ID: 1VPP) and EGFR (PDB ID: 1M17) were given. This process was done five times for each ligand. The product files of this code were the log files in text format and the output files in PDBQT format for the simulation. After the computation, the output and protein files (in PDBQT format) were exported to PyMol for the 3D simulation. UCSF Chimera, and PyMOL were used to visually show the docking process between proteins and ligands.

RESULTS

Methyl thiol tetrazolium (MTT) Assay Results

The results for the anticancer properties of the different concentrations of Atis (*Annona squamosa Linn.*) Seed Extract (12.5, 25, 50, & 100 µg/ml) and the Doxorubicin on the A549 Human Lung Adenocarcinoma are presented in Table 2 and 3. The inhibition of the samples on the human cell lines was determined by MTT Assay.

Table 2. *% Inhibition of Atis Seed Extract*

Extract concentration (µg/ml)	Percent Inhibition					
	n	T1	T2	T3	T4	Ave. ± SD
100	3	99.8 ± 0.35	99.2 ± 0.35	99.3 ± 0.47	99.8 ± 0.43	99.5 ± 0.40
50	3	62.7 ± 9.24	42.7 ± 4.90	43.1 ± 1.87	40.4 ± 6.06	47.2 ± 5.52
25	3	41.0 ± 3.50	19.7 ± 2.36	41.5 ± 3.11	22.6 ± 8.79	31.2 ± 4.44
12.5	3	34.4 ± 12.96	18.4 ± 2.66	41.2 ± 2.09	19.2 ± 2.16	28.3 ± 5.69
IC**50** (µg/mL)		35.34	56.44	56.16	36.55	46.12

The concentrations of the four trials were calculated for their medians and standard deviations, which shows the average of the different concentrations. For Trial 1, the inhibition for 100 µg/ml is 99.8 ± 0.35, for 50 µg/ml is

ISSN No. 2321-2705 | DOI: 10.51244/IJRSI |Volume XII Issue II February 2025

62.7 ± 9.24, for 25 µg/ml is 41.0 ± 3.50, for 12.5 µg/ml is 34.4 ± 12.96. For Trial 2, 100 µg/ml is 99.2 ± 0.35,for 50µg/ml is 42.7 ± 4.90,for 25µg/ml is 19.7 ± 2.36, for 12.5 µg/ml is 18.4 ± 2.66. For Trial 3, 100 µg/ml is 99.3 ± 0.47,for 50 µg/ml is 43.1 ± 1.87, for 25 µg/ml is 41.5 ± 3.11, for 12.5 µg/m; is 41.2 ± 2.09. For Trial 4, the percent inhibition of the concentration 100 µg/ml is 99.8 ± 0.43, for 50 µg/ml is 40.4 ± 6.06, for 25 µg/ml is 22.6 ± 8.79, for 12.5 µg/ml is 19.2 ± 2.16. The average of the four trials and the average of their standard deviation are as follows: 100 µg/ml is 99.5 ± 0.40, for 50 µg/ml is 47.2 ± 5.52, for 25 µg/ml is 31.2 ± 4.44, for 12.5 µg/ml is 28.3 ± 5.69. The IC50 for Trial 1 is 35.34, for Trial 2 is 56.44, for Trial 3 is 56.16 and Trial 4 is 46.12.

Table 3. *% Inhibition of Doxorubicin*

Extract concentration (µg/ml)	Percent Inhibition					
	n	T1	T2	T3	T4	Ave. ± SD
2	3	99.6 ± 0.13	99.6 ± 0.07	99.6 ± 0.09	99.2 ± 0.29	99.5 ± 0.15
1	3	88.5 ± 14.1	96.3 ± 0.55	93.4 ± 0.86	92.9 ± 1.70	92.8 ± 4.30
0.5	3	71.2 ± 4.37	74.5 ± 3.09	63.2 ± 1.34	59.7 ± 2.18	67.2 ± 2.75
0.25	3	42.7 ± 5.35	48.9 ± 4.93	45.7 ± 15.57	34.4 ± 1.42	42.9 ± 6.82
0.125	3	27.4 ± 7.69	33.9 ± 4.86	15.6 ± 4.41	21.6 ± 2.60	24.6 ± 4.89
IC**50** (µg/mL)		0.31	0.26	0.31	0.4	0.32

Comparatively, Table 10 shows the inhibition of doxorubicin against A549 Human Lung Adenocarcinoma in Trials 1,2,3 and 4. For Trial 1, the inhibition for 2 µg/ml is 99.6 ± 0.13, for 1 µg/ml is 88.5 ± 14.1, for 0.5 µg/ml is 71.2 ± 4.37, for 0.25 µg/ml is 42.7 ± 5.35, and for 0.125 µg/ml is 27.4 ± 7.69. For Trial 2, 2 µg/ml is 99.6 ± 0.07, for 1 µg/ml is 96.3 ± 0.55, for 0.5 µg/ml is 74.5 ± 3.09, for 0.25 µg/ml is 48.9 ± 4.93, and for 0.125 µg/ml is 33.9 ± 4.86. For Trial 3, 2 µg/ml is 99.6 ± 0.09, for 1 µg/ml is 93.4 ± 0.86, for 0.5 µg/ml is 63.2 ± 1.34, for 0.25 µg/ml is 45.7 ± 15.57, and for 0.125 µg/ml is 15.6 ± 4.41. For Trial 4, 2 µg/ml is 99.2 ± 0.29, for 1 µg/ml is 92.9 ± 1.70, for 0.5 µg/ml is 59.7 ± 2.18, for 0.25 µg/ml is 34.4 ± 1.42, and for 0.125 µg/ml is 21.6 ± 2.60. The average of the four trials and the average of their standard deviation are as follows: 2 µg/ml is 99.5 ±

ISSN No. 2321-2705 | DOI: 10.51244/IJRSI |Volume XII Issue II February 2025

0.15, for 1 µg/ml is 92.8 ± 4.30, for 0.5 µg/ml is 67.2 ± 2.75, for 0.25 µg/ml is 42.9 ± 6.82, and for 0.125 µg/ml is 24.6 ± 4.89. The IC50 of Trial 1,2,3 and 4 are 0.31, 0.26, 0.31 and 0.4 respectively.

Based on the previous tables, the Atis Seed Extract with the concentration of 100 µg/ml and the Doxorubicin with the concentration of 2 µg/ml showed the highest percent inhibition out of all the concentrations. Specifically, these two concentrations have similar standard deviations of 99.5 ± 0.40 µg/ml and 99.5 ± 0.15 µg/ml respectively. Below are the photomicrographs of the lung cancer cells after 72 hours exposure with the concentrations, which showed the similarities between them.

Figure 17. Photomicrograph of lung cancer cells after 72 h exposure with 2 µg/ml Doxorubicin.

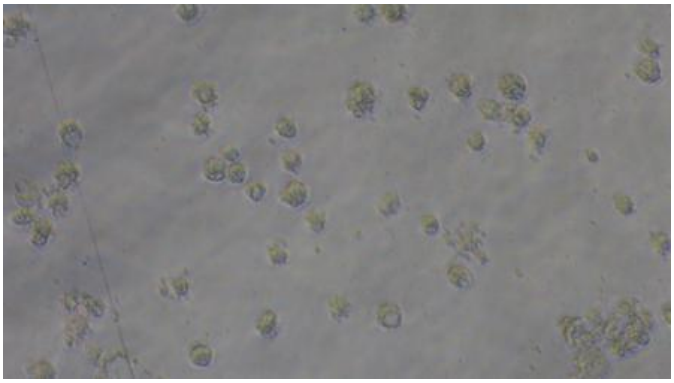

Figure 18. Photomicrograph of lung cancer cells after 72 h exposure with 100 µg/ml Atis Seed Extract.

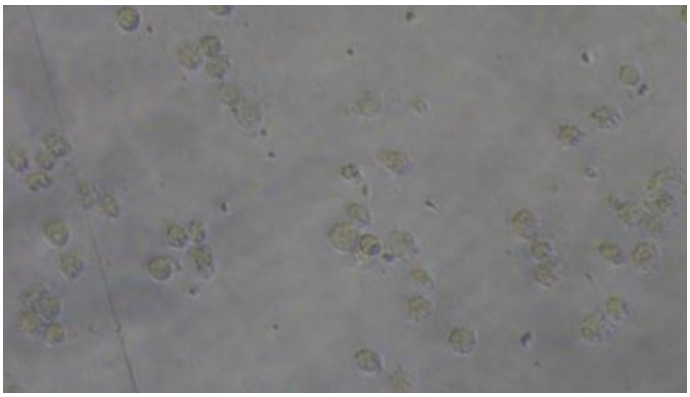

Figures 25, 26, 27, and 28 illustrate the half-maximal inhibitory concentrations (IC50) of Atis (Annona squamosa Linn.) across four independent trials. The IC50 values obtained were 35.34 in the first trial, 56.44 in the second trial, 56.16 in the third trial, and 36.55 in the fourth trial, resulting in an average IC50 value of 46.12 across all trials.

In comparison, the IC50 values for the doxorubicin control were 0.31 in the first trial, 0.26 in the second trial, 0.31 in the third trial, and 0.40 in the fourth trial, with an average IC50 value of 0.32 across the four trials.

Figure 19. IC50 of Atis Seed Extract (Trial 1)

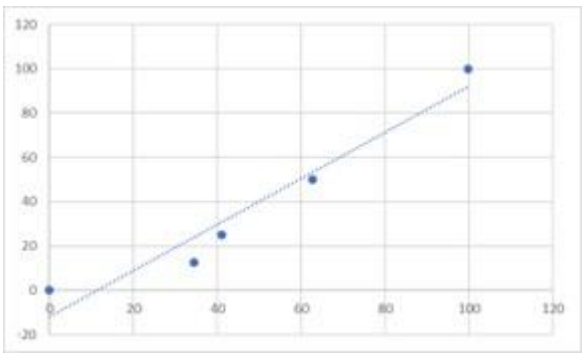

ISSN No. 2321-2705 | DOI: 10.51244/IJRSI |Volume XII Issue II February 2025

Figure 20. IC50 of Atis Seed Extract (Trial 2)

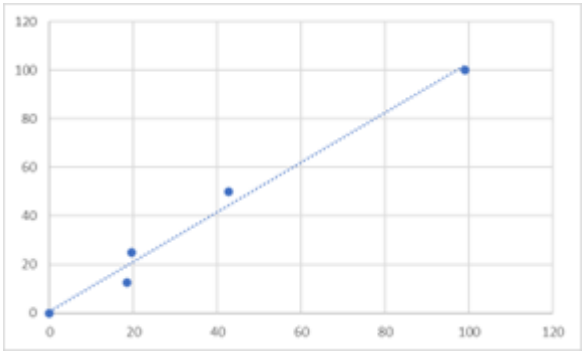

Figure 21. IC50 of Atis Seed Extract (Trial 3)

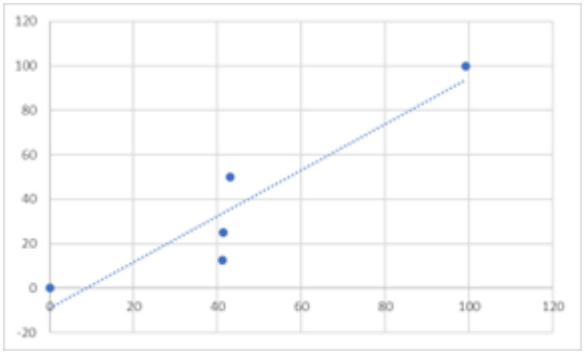

Figure 22. IC50 of Atis Seed Extract (Trial 4)

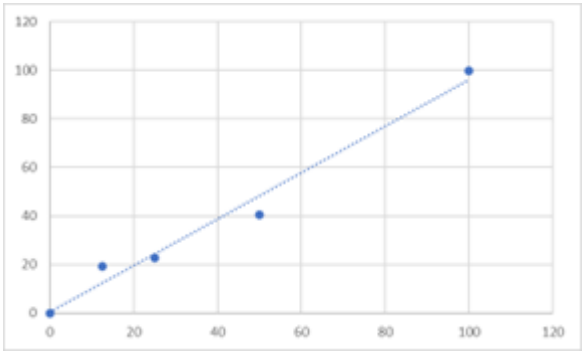

This study also analyzed the interactions between the *Annona squamosa Linn.* Seed bioactive compounds and the A549 Human Lung Adenocarcinoma receptors which are the VEGF (1VPP) and the EGFR (1M17). In line with this, the researchers evaluated the overall drug-likeness of the selected alkaloid phytochemicals under *Annona squamosa Linn.* After procuring the needed data, the researchers utilized the SMILES codes for each ligand to input in SwissADME and determine their physicochemical properties under Lipinski's Rule of 5 (Ro5).

Table 4. *Lipinski's Rule of 5 of the eleven ligands*

a	***b***	***c***	***d***	***e***	***f***
(2,4-cis- and trans)-bullatacinone	622.9	2	7	3.81	1
Annonacin A	596.9	4	7	3.46	1
Annonin VI	622.9	3	7	3.81	1
Annosquamosin A	362.5	1	4	3.35	0

ISSN No. 2321-2705 | DOI: 10.51244/IJRSI |Volume XII Issue II February 2025

Anonaine	265.3	1	3	2.83	0
Samoquasine A	196.2	1	2	2.13	0
Squamocin	622.9	3	7	3.81	1
Squamosinin A	622.9	3	8	2.85	1
Squamostatin C	638.9	4	8	3.02	1
Squamostatin D	622.9	3	7	3.81	1
Squamosten A	622.9	4	7	3.72	1

***a** = Ligands; **b** = Molecular Weight (g/mol, **<500 Da**); **c** = Number of Hydrogen bond donors (**<5**); **d** = Number of Hydrogen bond acceptors (**<10**); **e** = M Log $P_{o/w}$ (**≤4.15**); **f** = Number of Violations (**<2**)*

Among the eleven ligands presented in the above table, Annosquamosin A, Anonaine, and Samoquasine A were the ligands which did not violate any of the Lippinski's Rule of 5. (2,4-cis- and trans)-bullatacinone, Annonacin A, Annonin VI, Squamocin, Squamosinin A, Squamostatin C, Squamostatin D, and Squamosten A violated one rule which was the molecular weight. Nonetheless, the researchers proceeded with the 11 ligands because 1 violation was still considered, thus, the drug-likeness of the ligands was accepted.

PASS Prediction Results

Table 5. PASS Prediction of the eleven ligands including biological activities

a	***b***	***c***	***d***	***e***
(2,4-cis And trans)-bullatacinone	44584454	306	80	YES
Annonacin A	179866	542	128	YES
Annonin VI	130056	417	107	YES
Annosquamosin A	469215	283	76	YES
Anonaine	160597	321	91	YES
Samoquasine A	135465824	1802	406	YES
Squamocin	441612	401	108	YES
Squamosinin A	102153520	373	102	YES
Squamostatin C	180483	409	100	YES
Squamostatin D	9986398	529	133	YES
Squamosten A	102153564	458	124	YES

***a** = Ligands; **b** = CID Number; **c** = Total Number of Biological Activity Spectra; **d** = Number of **Pa > 0.3**; **e** = Contains Anticancer and Anti-Angiogenesis-related biological activities*

ISSN No. 2321-2705 | DOI: 10.51244/IJRSI |Volume XII Issue II February 2025

Above is the PASS prediction outcomes for ten ligands, highlighting their biological activities, specifically focusing on anticancer and anti-angiogenesis-related properties. Using the standardized threshold of Pa > 0.3 to predict biological activity spectra, these ligands were identified for their potential contributions to drug development targeting angiogenesis-related pathways, which are critical in processes such as cancer growth and metastasis.

Among the ligands, Samoquasine A stands out with the highest total number of biological activity spectra (1,802) and 406 predicted biological activities with Pa > 0.3, indicating its strong potential for multi-targeted applications, particularly in anti-angiogenesis-related functions. Similarly, other ligands, such as Annonacin A (542 biological activity spectra, 128 Pa > 0.3), Squamostatin D (529 spectra, 133 Pa > 0.3), and Squamosten A (458 spectra, 124 Pa > 0.3), also show substantial biological activity, suggesting their promise as candidates in further research on anti-angiogenesis treatments.

Moreover, all ten ligands exhibit activity associated with anticancer and anti-angiogenesis, a crucial attribute for cancer drug discovery, as inhibiting angiogenesis can prevent the growth of tumors by cutting off their blood supply. The presence of this activity across all ligands underscores their potential utility in therapies aimed at blocking blood vessel formation, thus restricting cancer progression.

ADMET Analysis Results

Table 6. ADMET Analysis (Absorption and Distribution)

a	***b***	***c***	***d***	***e***
LG-1	83.45%	0.591	1.46	78.43%
LG-2	70.52%	0.429	1.21	3.01%
LG-3	82.94%	0.549	1.43	14.71%
LG-4	96.92%	1.023	1.64	55.79%
LG-5	95.17%	1.721	2.30	61.87%
LG-6	94.32%	1.211	1.20	58.63%
LG-7	77.03%	0.535	1.48	82.23%
LG-8	83.54%	0.582	1.53	13.67%
LG-9	76.55%	0.471	1.08	73.97%
LG-10	82.27%	0.525	1.25	84.36%
LG-11	77.08%	0.452	1.45	73.71%

***a** = Ligand Number Codes; **b** = Human Intestinal Absorption; **c** = Caco-2 Permeability; **d** = Steady State Volume of Distribution; **e** = Plasma Protein Binding*

The ligands demonstrated varying degrees of Human Intestinal Absorption (HIA), with most ligands showing promising absorption rates above 70%. Notably, LG-4 exhibited the highest HIA at 96.92%, indicating strong potential for bioavailability when administered orally. Conversely, LG-2 showed the lowest HIA at 70.52%, suggesting reduced efficiency in absorption.

ISSN No. 2321-2705 | DOI: 10.51244/IJRSI |Volume XII Issue II February 2025

The Caco-2 permeability values of these ligands ranged from 0.429 to 1.721, all within the acceptable range for effective drug absorption. A Caco-2 permeability value above 1.0 is generally considered indicative of favorable absorption characteristics. This supports the notion that these ligands could be effectively absorbed through the intestinal barrier.

The Steady State Volume of Distribution (Vd) varied among the ligands, indicating differences in their distribution within the body. Most ligands presented a volume of distribution between 1.08 to 2.30 L/kg, reflecting a moderate distribution throughout tissues. Higher Vd values can indicate a greater ability to distribute into tissues, which can be advantageous for therapeutic effects.

Plasma Protein Binding percentages varied significantly, with LG-2 showing a notably low binding percentage of 3.01%, suggesting high free drug concentrations in circulation. In contrast, LG-1 and LG-7 exhibited higher plasma protein binding percentages at 78.43% and 82.23%, respectively. High protein binding can influence the bioavailability and therapeutic efficacy of a drug, as only the unbound fraction is pharmacologically active.

Table 7. ADMET Analysis (Metabolism, Excretion, and Toxicity)

a	***b***	***c***	***d***	***e***
LG-1	Medium Confidence Inhibitor	1.52	Safe	Safe
LG-2	Low Confidence Non-Inhibitor	1.81	Safe	Safe
LG-3	Low Confidence Non-Inhibitor	1.67	Safe	Safe
LG-4	Low Confidence Non-Inhibitor	0.51	Safe	Safe
LG-5	Medium Confidence Inhibitor	1.11	Safe	Safe
LG-6	High Confidence Inhibitor	0.63	Safe	Safe
LG-7	Medium Confidence Inhibitor	1.67	Safe	Safe
LG-8	Low Confidence Non-Inhibitor	1.50	Safe	Safe
LG-9	Medium Confidence Inhibitor	1.69	Safe	Safe
LG-10	Medium Confidence Inhibitor	1.67	Safe	Safe
LG-11	Medium Confidence Inhibitor	1.84	Safe	Safe

***a** = Ligand Number Codes; **b** = CYP3A4 Inhibitor; **c** = Total Clearance; **d** = AMES Toxicity; **e** = Carcinogenesis*

The ligands exhibit varying classifications as CYP450 inhibitors. Ligands LG-1, LG-5, LG-6, LG-7, LG-9, LG-10, and LG-11 were identified as inhibitors, with LG-6 classified as a high confidence inhibitor. The inhibition of CYP450 is significant as it plays a crucial role in drug metabolism; thus, understanding the potential for interaction with other drugs is essential for therapeutic safety.

The total clearance rates for these ligands ranged from 0.51 to 1.84 L/h. Notably, LG-4 had the lowest clearance rate at 0.51 L/h, indicating a slower elimination from the body, while LG-11 exhibited the highest clearance at 1.84 L/h. Total clearance is a critical factor in determining drug dosing and frequency, as it informs how quickly a compound is removed from systemic circulation.

All ligands were assessed for AMES toxicity and carcinogenic potential, with results indicating that they are all

ISSN No. 2321-2705 | DOI: 10.51244/IJRSI |Volume XII Issue II February 2025

classified as "Safe." This suggests that these compounds are not expected to pose significant genotoxic risks or contribute to cancer development, highlighting their suitability for further exploration in pharmacological applications.

Overall, the data underscores the varied metabolic profiles and safety profiles of the ligands, which are crucial for determining their viability in drug development and therapeutic contexts.

Molecular Docking Results

Table 8. Binding Affinity Scores of the eleven Annona Squamosa Linn. ligands and the VEGF (1VPP)

a	***b***
(2,4-cis- and trans)-bullatacinone	-7.0
Annonacin A	-6.6
Annosquamosin A	-6.8
Annonin VI	-6.8
Anonaine	-7.2
Samoquasine A	-6.9
Squamocin	-6.4
Squamosinin A	-6.9
Squamostatin C	-6.9
Squamostatin D	-6.0
Squamosten A	-5.8

***a** = Ligands + FDA-approved Post-Attachment Inhibitor and **b** = Binding Affinity Scores (kcal/mol)*

Table 8 displayed the binding affinity scores of the eleven *Annona squamosa Linn.* ligands and the Vascular Endothelial Growth Factor (VEGF). The binding affinity scores indicate and quantify the strength of the interaction between the ligand and the protein. The score is expressed through kcal/mol. A lower kcal/mol signifies a higher affinity meaning the ligand binds more strongly, while a higher kcal/mol indicates weaker binding (Öztürk et al., 2018).

Anonaine showed the highest affinity having a score of -7.2 kcal/mol, followed by (2,4-cis- and trans)-bullatacinone with a score of -7.0 kcal/mol, Samoquasine A, Squamosinin A, and Squamostatin C with a score of -6.9, Annosquamosin A and Annonin VI has -6.8 kcal/mol, Annonacin A has -6.6 kcal/mol, Squamocin has -6.4 kcal/mol, and Squamostatin D has -6.0 kcal/mol. Squamosten A ranked last with a score of -5.8 kcal/mol, indicating weaker binding.

Table 9. Binding Affinity Scores of the eleven Annona Squamosa Linn. ligands and the EGFR (1M17)

a	***b***
(2,4-cis- and trans)-bullatacinone	-7.1

ISSN No. 2321-2705 | DOI: 10.51244/IJRSI |Volume XII Issue II February 2025

Annonacin A	-6.9
Annosquamosin A	-7.2
Annonin VI	-6.8
Anonaine	-9.2
Samoquasine A	-7.4
Squamocin	-6.5
Squamosinin A	-7.1
Squamostatin C	-7.5
Squamostatin D	-7.0
Squamosten A	-7.0

***a** = Ligands + FDA-approved Post-Attachment Inhibitor and **b** = Binding Affinity Scores (kcal/mol)*

Table 9 displayed the binding affinity scores of the eleven *Annona squamosa Linn.* ligands and the Epidermal Growth Factor Receptor (EGFR) protein. The binding affinity scores reflect and measure the strength of the interaction between the ligand and the protein, expressed in kcal/mol. A lower kcal/mol value indicates a stronger binding affinity, meaning the ligand binds more tightly, whereas a higher kcal/mol value signifies weaker binding (Öztürk et al., 2018).

Anonaine showed the highest affinity having a score of -9.2 kcal/mol, followed by Squamostatin C with a score of -7.5 kcal/mol, Samoquasine A with a score of -7.4, Annosquamosin A has -7.2 kcal/mol, (2,4-cis- and trans)-bullatacinone and Squamosinin A has -7.1 kcal/mol, Squamostatin D and Squamosten A has -7.0 kcal/mol, Annonacin A has -6.9 kcal/mol, Annonin VI has -6.8 kcal/mol, and Squamocin ranked last with a score of -6.5 kcal/mol.

Visualization of the Top Two Phytochemicals with the Most Interacting Residues

Figure 23. ***Anonaine-VEGF complex. Chimera 3D visualization***

ISSN No. 2321-2705 | DOI: 10.51244/IJRSI |Volume XII Issue II February 2025

Figure 24. ***(2,4-cis- and trans)-bullatacinone-VEGF complex. Chimera 3D visualization***

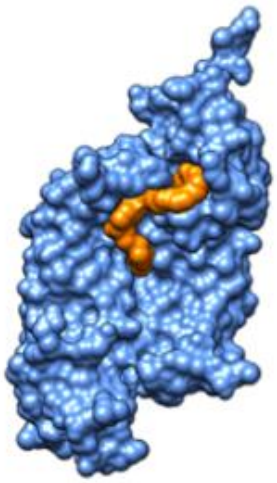

Figure 25. ***Anonaine-EGFR complex. Chimera 3D visualization***

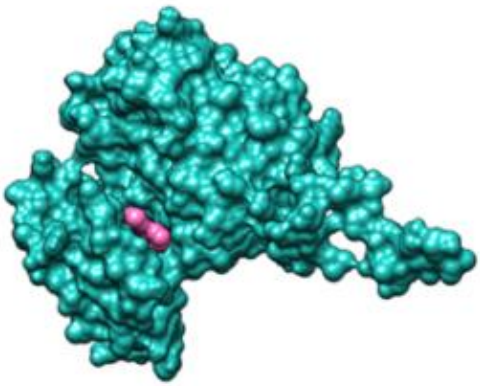

Figure 26. ***Squamostatin C-EGFR complex. Chimera 3D visualization***

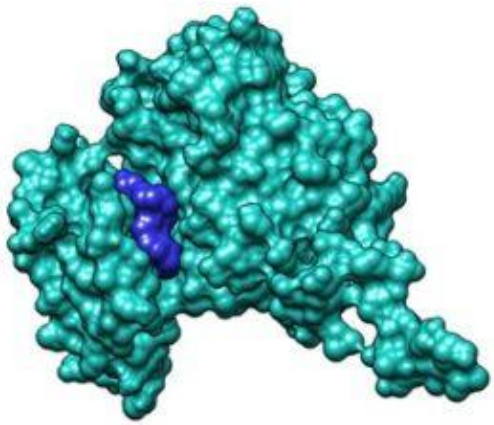

DISCUSSION

Methyl thiol tetrazolium (MTT) Assay Discussion

The present study evaluated the potential of Annona squamosa Linn. (Atis) seed extract against A549 lung cancer cells, confirming the presence of key phytochemicals such as flavonoids, alkaloids, and saponins—compounds

ISSN No. 2321-2705 | DOI: 10.51244/IJRSI |Volume XII Issue II February 2025

known for their anticancer properties (Vama & Cherekar, 2020). These may inhibit cell proliferation by arresting the cell cycle (Ohiagu et al., 2021).

Atis seed extract was tested at concentrations ranging from 12.5 to 100 µg/ml, with the highest concentration (100 µg/ml) achieving 99.5% inhibition. The IC50 values across four trials ranged from 35.34 to 56.44 µg/ml, with 35.34 µg/ml being the most effective. These results suggest the extract's strong anticancer potential, aligning with findings from Amaani and Dwira (2018) on Glycine soja ethanol extract.

The IC50 value is a key pharmacological parameter indicating the concentration needed to inhibit 50% of cell growth; a lower IC50 reflects higher potency (Sebaugh, 2011). Variations in IC50 may result from differences in extract composition, experimental conditions, or cell behavior.

Comparisons with doxorubicin, a widely used chemotherapeutic agent, highlight the extract's potential as a natural alternative with possibly fewer side effects (Jain et al., 2021). Doxorubicin disrupts DNA replication and induces apoptosis by inhibiting topoisomerase II (Thorn et al., 2011).

The study suggests that Annona squamosa extract exerts its anticancer effects through ROS generation and apoptosis induction, activating caspases 3 and 9, crucial for programmed cell death (Tian et al., 2020; Javed et al., 2021). This aligns with existing research on plant-derived anticancer comp**o**unds (Vama & Cherekar, 2020; Ohiagu et al., 2021). These findings support the potential of Annona squamosa as a promising therapeutic agent for lung cancer.

PASS Prediction Discussion

The PASS prediction results for eleven ligands highlight their potential anticancer and anti-angiogenic activities, essential for drug discovery and cancer treatment. Using a threshold of Pa > 0.3, the study emphasizes their role in inhibiting angiogenesis, a key factor in tumor growth and metastasis (Lagunin et al., 2011). Since tumors require a blood supply for survival, compounds that disrupt this process are promising candidates for cancer therapy.

Among the ligands, Samoquasine A shows exceptional potential, with 1,802 total biological activity spectra and 406 predicted activities with Pa > 0.3. Its broad activity profile suggests multi-target capabilities, crucial in addressing cancer's complex and adaptive nature (Filmonov et al., 2014). By inhibiting tumor vascularization, Samoquasine A aligns with findings on effective anti-angiogenic agents.

Other ligands, such as Annonacin A (542 spectra, 128 Pa > 0.3), Squamostatin D (529 spectra, 133 Pa > 0.3), and Squamosten A (458 spectra, 124 Pa > 0.3), also exhibit strong anti-angiogenic potential, warranting further investigation.

These findings reinforce the significance of plant-derived compounds in modern drug discovery, particularly in anti-angiogenesis research. Given their promising activity, these ligands merit further experimental validation as potential cancer therapies.

ADMET Discussion

The ADMET results indicate promising pharmacokinetic profiles for the ligands, particularly with most ligands showing Human Intestinal Absorption (HIA) above 70%, such as LG-4 with the highest HIA at 96.92%, while LG-2 exhibited the lowest at 70.52%, highlighting potential differences in bioavailability (Raju et al., 2021). Caco-2 permeability values also support efficient absorption, with several ligands exceeding the 1.0 threshold, indicative of favorable absorption characteristics (Raju et al., 2021).

Caco-2 permeability values, ranging from 0.429 to 1.721, indicate that ligands with values above 1.0 have favorable absorption characteristics, supporting their effectiveness when administered orally (Chandran et al., 2022).

The Steady State Volume of Distribution (Vd) results, ranging from 1.20 to 2.30 L/kg, show moderate

ISSN No. 2321-2705 | DOI: 10.51244/IJRSI |Volume XII Issue II February 2025

distribution throughout body tissues. Higher Vd values suggest that these ligands have a stronger ability to distribute beyond the bloodstream into various tissues, which is beneficial for achieving therapeutic concentrations at target sites. On the other hand, ligands like LG-2, with a low plasma protein binding percentage (3.01%), may remain highly bioavailable in circulation, increasing the potential for therapeutic effects at lower doses. In contrast, ligands with higher binding percentages, such as LG-1 and LG-7, might require adjustments in dosing to ensure sufficient active drug remains unbound and pharmacologically effective (Chandran et al., 2022).

Moreover, CYP450 inhibition, observed in multiple ligands such as LG-6, raises important considerations for metabolism and drug interactions. CYP450 is a key enzyme in drug metabolism, and its inhibition can lead to slower clearance of co-administered drugs, potentially causing toxicity. Understanding this interaction is critical when developing these ligands into safe therapeutics (Raju et al., 2021).

Clearance rates, ranging from 0.51 to 1.84 L/h, provide insight into the elimination efficiency of these ligands. LG-4's low clearance rate suggests a longer presence in the body, which may reduce the frequency of dosing, whereas LG-11's high clearance rate points to faster elimination, potentially necessitating more frequent administration to maintain therapeutic levels.

Molecular Docking Discussion

The Atis seed extract contains 29 phytochemicals; however, only 21 ligands were found in the PubChem database. The SMILES representation of each ligand was then evaluated using SwissADME (http://www.swissadme.ch/), an online tool that assesses the drug-likeness of phytochemicals. The primary function of SwissADME is to offer unrestricted access to various parameters and predictive models for determining physicochemical properties, as well as estimating pharmacokinetics, drug-likeness, and medicinal chemistry compatibility of small molecules (SwissADME, n.d.). According to Lipinski's Rule of Five, only the phytochemicals who had violations of less than two passed the drug-likeness test (Karami et al., 2021). Among the 21 ligands evaluated, only 11 phytochemicals met the criteria outlined by Lipinski's Rule of Five. These 11 phytochemicals were subsequently analyzed through molecular docking.

Through the molecular docking process, the researchers were able to find the different binding affinities of each ligand with the two different proteins VEGF (1VPP) and EGFR (1M17). The results of the molecular docking between the VEGF protein (1VPP) and the 11 different ligands ranged from -5.8 to -7.2 kcal/mol. The top two ligands with the lowest binding affinity with 1VPP are Anonaine and (2,4-cis- and trans)-bullatacinone, with -7.2 kcal/mol and -7.0 kcal/mol respectively. While for the EGFR protein (1M17), the results ranged from -6.8 to -9.2 kcal/mol, with Anonaine having the lowest binding affinity of -9.2 kcal/mol followed by Squamostatin C with -7.5 kcal/mol. A lower binding affinity value signifies a stronger interaction, which is crucial for the design of drugs that selectively target specific biomolecules (Malvern Panalytical, n.d.). According to Spassov (2024), binding affinity is characterized as a fundamental parameter in drug design, indicating the strength of the interaction between a molecule and its target protein. The phytochemicals which had a binding affinity less than -6.9 (<-6.9) and part of the top two lowest binding affinity are (2,4-cis- and trans)-bullatacinone, Anonaine, and Squamostatin C, the three phytochemicals are Acetogenines. In a study by Jacobo-Herrera et al. (2019), Acetogenins are versatile anticancer agents that induce tumor cell death through multiple mechanisms. They have the ability to modulate the efflux of chemotherapeutic drugs from cancer cells and are potent inducers of apoptosis. Their bioactive versatility is demonstrated by their capacity to regulate the cell cycle by arresting cells in the G1 phase, promote apoptosis through the inhibition of various proteins, and even induce autophagy.

CONCLUSION AND RECOMMENDATION

This study demonstrates the anticancer activity and angiogenic inhibition of Atis *(Annona squamosa Linn.)* Seed Extract against A549 Human Lung Adenocarcinoma, through MTT Assay and Molecular Docking Analyses. The MTT Assay results showed that the Atis Seed Extract displayed great potential anticancer activity comparable to Doxorubicin, a chemotherapy drug, considering that the variable used in the study was pure crude extract. The 12.5 µg/ml concentration showed the weakest inhibition. Meanwhile, the 100 µg/ml crude extract exhibited the most potent anticancer activity against the A549 Human Lung Adenocarcinoma. In conclusion,

low concentrations of the Atis Seed Extract showed low anticancer activity while higher concentrations displayed more formidable anticancer activity against the A549 cell line.

As for the Molecular Docking, the Anonaine ligand showed the lowest binding affinity score of -7.2 kcal/mol, followed by (2,4-cis- and trans)-bullatacinone with a score of -7.0 kcal/mol, when binded with the VEGF protein. Meanwhile, for the EGFR, the Anonaine ligand still showed the lowest binding affinity score of -9.2 kcal/mol, followed by Squamostatin C which has a binding affinity of -7.5 kcal/mol. This indicates that Anonaine, (2,4-cis- and trans)-bullatacinone, and Squamostatin C have the strongest binding affinity and are potentially crucial ingredients for effective drug-target interactions, enhancing therapeutic efficacy.

These findings indicate the potential of the Atis Seed Extract for future research exploring their therapeutic applications, however, several recommendations are suggested to enhance the study. Notably, it is essential to validate the findings through in vivo experiments, as this could assess and provide a better understanding of its therapeutic potential and safety profile. Furthermore, it is suggested to explore different techniques like encapsulating the extract in nanoparticles, to enhance bioavailability of the extract. In summary, these recommendations are crucial in achieving the true capability of the study in discovering new treatments and potential applications in the clinical environment.

REFERENCES

1. Roser, M., & Ritchie, H. (2024, March 12). *Cancer*. Our World in Data. https://ourworldindata.org/cancer#note-1
2. Dee, E. C., Ang, C. D. U., Ting, F. I. L., Tangco, E. D., & Eala, M. a. B. (2022). Improving cancer care in the Philippines: The need for deliberate and careful implementation of the National Integrated Cancer Control Act. *The Lancet Regional Health - Western Pacific*, *28*, 100615. https://doi.org/10.1016/j.lanwpc.2022.100615
3. Bray, F., Laversanne, M., Sung, H., Ferlay, J., Siegel, R. L., Soerjomataram, I., & Jemal, A. (2024). Global cancer statistics 2022: GLOBOCAN estimates of incidence and mortality worldwide for 36 cancers in 185 countries. *CA a Cancer Journal for Clinicians*, *74*(3), 229–263. https://doi.org/10.3322/caac.21834
4. Suanes, P. N., Alberto, N. R. I., Alberto, I. R. I., Swami, N., Eala, M. a. B., Tangco, E. D., & Dee, E. C. (2023). Lung cancer screening in the Philippines: the need for guidelines based on the local context and the imperative for improved access to screening. *The Lancet Regional Health - Western Pacific*, *32*, 100704. https://doi.org/10.1016/j.lanwpc.2023.100704
5. *Types of lung cancer: common, rare, aggressive & more*. (n.d.). City of Hope. https://www.cancercenter.com/cancer-types/lung-cancer/types
6. *Angiogenesis inhibitors*. (2018, April 2). Cancer.gov. https://www.cancer.gov/about-cancer/treatment/types/immunotherapy/angiogenesis-inhibitors-fact-sheet
7. Bonvissuto, D. (2024, June 14). *Is there a cure for cancer?* WebMD. https://www.webmd.com/cancer/cure-for-cancer
8. Asiimwe, J. B., Nagendrappa, P. B., Atukunda, E. C., Kamatenesi, M. M., Nambozi, G., Tolo, C. U., Ogwang, P. E., & Sarki, A. M. (2021). Prevalence of the Use of Herbal Medicines among Patients with Cancer: A Systematic Review and Meta-Analysis. *Evidence-based Complementary and Alternative Medicine*, *2021*, 1–18. https://doi.org/10.1155/2021/9963038
9. Vyas, K., Manda, H., Sharma, R. K., & Singhal, G. (2012). An update review on Annona Squamosa. *IJPT*, *3*(2), 107-118.
10. Chen, J., Chen, Y., & Li, X. (2011). Beneficial Aspects of Custard Apple (Annona squamosa L.) Seeds. In *Elsevier eBooks* (pp. 439–445). https://doi.org/10.1016/b978-0-12-375688-6.10052-0
11. Amaani, R., & Dwira, S. (2018). Phytochemical content an in vitro toxicity of Glycine soja ethanol extract on the A549 Lung cancer line cell. *Journal of Physics Conference Series*, *1073*, 032042. https://doi.org/10.1088/1742-6596/1073/3/032042
12. Van Meerloo, J., Kaspers, G. J. L., & Cloos, J. (2011). Cell sensitivity assays: the MTT assay. *Methods in Molecular Biology*, 237–245. https://doi.org/10.1007/978-1-61779-080-5_20
13. Lagunin, A. A., Goel, R. K., Gawande, D. Y., Pahwa, P., Gloriozova, T. A., Dmitriev, A. V., Ivanov, S. M., Rudik, A. V., Konova, V. I., Pogodin, P. V., Druzhilovsky, D. S., & Poroikov, V. V. (2014). Chemo-

and bioinformatics resources for in silico drug discovery from medicinal plants beyond their traditional use: a critical review. *Natural Product Reports*, *31*(11), 1585–1611. https://doi.org/10.1039/c4np00068d
14. Raju, L., Lipin, R., & Eswaran, R. (2021). Identification, ADMET evaluation and molecular docking analysis of Phytosterols from Banaba (Lagerstroemia speciosa (L.)Pers) seed extract against breast cancer. *In Silico Pharmacology*, *9*(1). https://doi.org/10.1007/s40203-021-00104-y
15. Dar, A. M., & Mir, S. (2017). Molecular docking: approaches, types, applications and basic challenges. *Journal of Analytical & Bioanalytical Techniques*, *08*(02). https://doi.org/10.4172/2155-9872.1000356
16. Vyas, K., Manda, H., Sharma, R. K., & Singhal, G. (2012). An update review on Annona Squamosa. *IJPT*, *3*(2), 107-118.
17. Ribatti, D. (2017). The chick embryo chorioallantoic membrane (CAM) assay. *Reproductive Toxicology*, *70*, 97–101. https://doi.org/10.1016/j.reprotox.2016.11.004
18. Acda, M. N. (2014). Chemical composition of ethanolic seed extract of Annona squamosa L. and A. muricata L.(Annonaceae) using GC-MS analysis. *Philippine Agricultural Scientist*, *97*(4), 422-426.8
19. Pandey, N., & Barve, D. (2011). Phytochemical and pharmacological review on Annona squamosa Linn. *International Journal of research in pharmaceutical and biomedical sciences*, *2*(4), 1404-1412.
20. Karami, T. K., Hailu, S., Feng, S., Graham, R., & Gukasyan, H. J. (2021). Eyes on Lipinski's Rule of Five: a new "Rule of Thumb" for physicochemical design space of ophthalmic drugs. *Journal of Ocular Pharmacology and Therapeutics*, *38*(1), 43–55. https://doi.org/10.1089/jop.2021.0069
21. Tijjani, H., Olatunde, A., Adegunloye, A. P., & Ishola, A. A. (2022). In silico insight into the interaction of 4-aminoquinolines with selected SARS-CoV-2 structural and nonstructural proteins. In *Elsevier eBooks* (pp. 313–333). https://doi.org/10.1016/b978-0-323-95578-2.00001-7
22. Tuli, H. S., Sharun, K., Dhama, K., Bansal, P., Bhatia, G., Kumar, M., & Abbas, Z. (2022). In Silico evaluation of Myricetin, Fisetin, and Genistein as glycoprotein inhibitors: Hope for the Discovery of Anti-Nipah Virus Agents. *Indian Vet J*, *99*(01), 24-30.
23. Ali, M. H., Anwar, S., Roy, P. K., & Ashrafuzzaman, M. (2018). Virtual screening for identification of small lead compound inhibitors of Nipah virus attachment glycoprotein. *J Pharmacog Pharmacopro*, *9*. https://doi.org/10.4172/2153-0645.1000180
24. Öztürk, H., Özgür, A., & Ozkirimli, E. (2018). DeepDTA: deep drug–target binding affinity prediction. *Bioinformatics*, *34*(17), i821–i829. https://doi.org/10.1093/bioinformatics/bty593
25. Vama, L. A. P. S. I. A., & Cherekar, M. N. (2020). Production, extraction and uses of eco-enzyme using citrus fruit waste: wealth from waste. *Asian Jr. of Microbiol. Biotech. Env. Sc*, *22*(2), 346-351.
26. Ohiagu, F. O., Chikezie, P. C., Chikezie, C. M., & Enyoh, C. E. (2021). Anticancer activity of Nigerian medicinal plants: a review. *Future Journal of Pharmaceutical Sciences*, *7*(1). https://doi.org/10.1186/s43094-021-00222-6
27. Amaani, R., & Dwira, S. (2018). Phytochemical content an in vitro toxicity of Glycine soja ethanol extract on the A549 Lung cancer line cell. *Journal of Physics Conference Series*, *1073*, 032042. https://doi.org/10.1088/1742-6596/1073/3/032042
28. Sebaugh, J. L. (2010). Guidelines for accurate EC50/IC50 estimation. *Pharmaceutical Statistics*, *10*(2), 128–134. https://doi.org/10.1002/pst.426
29. Jain, N., Jain, P., Rajput, D., & Patil, U. K. (2021). Green synthesized plant-based silver nanoparticles: therapeutic prospective for anticancer and antiviral activity. *Micro and Nano Systems Letters*, *9*(1). https://doi.org/10.1186/s40486-021-00131-6
30. Thorn, C. F., Oshiro, C., Marsh, S., Hernandez-Boussard, T., McLeod, H., Klein, T. E., & Altman, R. B. (2010). Doxorubicin pathways. *Pharmacogenetics and Genomics*, *21*(7), 440–446. https://doi.org/10.1097/fpc.0b013e32833ffb56
31. Tian, S., Saravanan, K., Mothana, R. A., Ramachandran, G., Rajivgandhi, G., & Manoharan, N. (2020). Anti-cancer activity of biosynthesized silver nanoparticles using Avicennia marina against A549 lung cancer cells through ROS/mitochondrial damages. *Saudi Journal of Biological Sciences*, *27*(11), 3018–3024. https://doi.org/10.1016/j.sjbs.2020.08.029
32. Javed, B., Ikram, M., Farooq, F., Sultana, T., Mashwani, Z., & Raja, N. I. (2021). Biogenesis of silver nanoparticles to treat cancer, diabetes, and microbial infections: a mechanistic overview. *Applied Microbiology and Biotechnology*, *105*(6), 2261–2275. https://doi.org/10.1007/s00253-021-11171-8
33. Kumari, S., Kumari, P., Panda, P. K., Patel, P., Jha, E., Mallick, M. A., Suar, M., & Verma, S. K. (2020). Biocompatible Biogenic Silver Nanoparticles Interact with Caspases on An Atomic Level to Elicit

Apoptosis. *Nanomedicine*, *15*(22), 2119–2132. https://doi.org/10.2217/nnm-2020-0138
34. *SwissADME*. (n.d.). http://www.swissadme.ch/faq.php
35. Karami, T. K., Hailu, S., Feng, S., Graham, R., & Gukasyan, H. J. (2021). Eyes on Lipinski's Rule of Five: a new "Rule of Thumb" for physicochemical design space of ophthalmic drugs. *Journal of Ocular Pharmacology and Therapeutics*, *38*(1), 43–55. https://doi.org/10.1089/jop.2021.0069
36. Malvern Panalytical. (n.d.). *Binding affinity*. https://www.malvernpanalytical.com/en/products/measurement-type/binding-affinity
37. Spassov, D. S. (2024). Binding Affinity Determination in Drug Design: Insights from Lock and Key, Induced Fit, Conformational Selection, and Inhibitor Trapping Models. *International Journal of Molecular Sciences*, *25*(13), 7124. https://doi.org/10.3390/ijms25137124
38. Jacobo-Herrera, N., Pérez-Plasencia, C., Castro-Torres, V. A., Martínez-Vázquez, M., González-Esquinca, A. R., & Zentella-Dehesa, A. (2019). Selective acetogenins and their potential as anticancer agents. *Frontiers in Pharmacology*, *10*. https://doi.org/10.3389/fphar.2019.00783
39. Shi, Z., Chen, J., Guo, X., Cheng, L., Guo, X., & Yu, T. (2018). In silico identification of potent small molecule inhibitors targeting epidermal growth factor receptor 1. *Journal of Cancer Research and Therapeutics*, *14*(1), 18–23. https://doi.org/10.4103/jcrt.jcrt_365_17
40. Chen, D., Oezguen, N., Urvil, P., Ferguson, C., Dann, S. M., & Savidge, T. C. (2016). Regulation of protein-ligand binding affinity by hydrogen bond pairing. *Science Advances*, *2*(3). https://doi.org/10.1126/sciadv.1501240
41. Lagunin, A., Filimonov, D., & Poroikov, V. (2010). Multi-Targeted Natural Products Evaluation Based on Biological Activity Prediction with PASS. *Current Pharmaceutical Design*, *16*(15), 1703–1717. https://doi.org/10.2174/138161210791164063
42. Filimonov, D. A., Lagunin, A. A., Gloriozova, T. A., Rudik, A. V., Druzhilovskii, D. S., Pogodin, P. V., & Poroikov, V. V. (2014). Prediction of the biological activity spectra of organic compounds using the PASS online web resource. *Chemistry of Heterocyclic Compounds*, *50*(3), 444–457. https://doi.org/10.1007/s10593-014-1496-1
43. Chandran, K., Shane, D. I., Zochedh, A., Sultan, A. B., & Kathiresan, T. (2022). Docking simulation and ADMET prediction based investigation on the phytochemical constituents of Noni (Morinda citrifolia) fruit as a potential anticancer drug. *In Silico Pharmacology*, *10*(1). https://doi.org/10.1007/s40203-022-00130-4